Available online at www.sciencedirect.com
SCIENCE DIRECT®
Bioelectrochemistry 60 (2003) 97–106
Bioelectrochemistry
www.elsevier.com/locate/bioelechem

Modeling of ionic relaxation around a biomembrane disk

László Oroszi[a,*], Olaf Hasemann[b], Elmar Wolff[b], András Dér[a]

[a] *Institute of Biophysics of the Hungarian Academy of Sciences, Temesvári krt. 62, H-6701, P.O. Box 521, H-6726 Szeged, Hungary*
[b] *Institut für Angewandte Biotechnologie und Systemanalyse, Witten, Germany*

Received 14 June 2002; received in revised form 14 February 2003; accepted 19 May 2003

Abstract

A simplified Brownian dynamics model and the corresponding software implementation have been developed for the simulation of electrolyte dynamics on the mesoscopic scale. In addition to direct control simulations, the model system has been verified by a quantitative comparison with the Debye–Hückel theory. As a first application, the model was used to simulate ionic relaxation processes following abrupt intramembrane charge rearrangements in the case of a disk shaped membrane. In addition to its general implications, the obtained properties of the relaxation kinetics confirm the assumptions of the theory of the so-called suspension method, a technique capable of tracing molecular charge motions of membrane proteins in three dimensions.

Keywords: Brownian dynamics; Ionic relaxation; Diffuse double layer; Bacteriorhodopsin

1. Introduction

The interface of biological membranes and the surrounding electrolyte is the location of important signal and energy transduction processes. Studies of the lateral organization of cell membranes revealed that proteins and lipids tend to form supramolecular assemblies as stable or temporary mesoscopic structures interacting with different ligands and the electrolyte. The available experimental and theoretical information is concerned mainly with the biochemical characterization of supramolecular assemblies, at the same time there are a relatively few attempts to model the electrostatics and the dynamic behaviour of the electrolyte on the mesoscopic scale.

There are basically three levels of theory to model the electrolyte in biological systems. The most fundamental and sophisticated approach is molecular dynamics (MD) that is used mainly for modeling individual proteins and their microenvironment. Towards systems having larger dimensions, theories of higher phenomenological levels: Brownian dynamics (BD) and continuum theories can be used.

During the past years, molecular dynamics modeling with explicit solvent and membranes have provided a substantial amount of information about a number of membrane proteins, mainly ion channels. In spite of the impressive increase in computational performance, MD calculations still face fundamental difficulties [1]. The main problem is that the duration of the physical processes to be modeled (e.g. ion transport) is usually far longer than that can be handled by MD.

Brownian dynamics represents an attractive way for simulating over long time scales without the need of handling the solvent molecules explicitly. In BD, stochastic equations of motions with effective forces are integrated utilizing the chaotic nature of ionic motion in water. By the application of BD simulations, a remarkable amount of information has been gathered about ion channels (e.g. Refs. [2–7]), macromolecular polyions and enzyme substrate interactions [8–10].

On the highest phenomenological level, there are the continuum theories of electrolytes originally developed for bulky systems early in the 20th century. Although the validity of continuum theories for the macroscopic scale has been proven by numerous experiments, the more recent problems in biology are usually concerned with mesoscopic systems. The reliability of continuum theories (Poisson–Boltzmann and Poisson–Nernst–Planck) in systems with dimensions comparable to the Debye length has been investigated lately [11,12]. Based on the comparison of these theories with BD simulations, it was concluded, that in systems having dimensions comparable or smaller than

* Corresponding author. Tel.: +36-62-432-232; fax: +36-62-433-133.
E-mail address: oroszi@nucleus.szbk.u-szeged.hu (L. Oroszi).

1567-5394/03/$ - see front matter © 2003 Elsevier B.V. All rights reserved.
doi:10.1016/S1567-5394(03)00052-5

the Debye length, continuum theories fail to yield reliable estimates.

Our approach was to define and implement a simplified Brownian dynamics model on the mesoscopic scale. Tracing of individual ion trajectories is based on a special case of the Langevin equation, corresponding to the situation of frequent collisions of ions with the solvent molecules compared to the simulation time step. In our approximation we neglect all specific short range or "chemical" interactions (such as Pauling and hydration forces between ions, surface adsorption effects). The membrane, the ions, and the simulation volume are treated as geometric objects. During simulations, in the case of ion–ion, ion–membrane and ion–wall (of the simulation volume) collisions, specific "low-cost" intersection handler algorithms are employed. Exploiting the computational benefits of these simplifications, we typically deal with time steps of approximately 250 ps and simulation volumes having a diameter in the range of 100 nm.

In this paper, first we introduce our model: we discuss the underlying physical concepts and briefly refer to the implementation, the possibilities of the simulation tool. This is followed by a comparison of the model and the Debye–Hückel theory. Then we apply the model to the problem of ionic relaxation as a consequence of abrupt intramembrane dipole transitions in the case of a membrane disk. In addition to its general implications concerning the dielectric properties of membrane fragments, solving this problem is essential for the interpretation of electric signals associated with intramolecular charge displacements of membrane proteins [13]. Such signals can be measured in three dimensions by the so-called suspension method [14] as it was demonstrated experimentally on bacteriorhodopsin (bR) containing purple membrane fragments [15]. Our simulations are in concert with earlier assumptions based on experimental data [16] and reveal new information on the kinetics of the relaxation process.

2. Theoretical methods

2.1. Brownian dynamics for electrolytes

According to the BD framework, the electrolyte is modeled by calculating all ion trajectories separately based on a stochastic equation of motion. This is called the Langevin equation that can be written in the following form for the ith ion:

$$m_i \frac{\mathrm{d}^2 \vec{r_i}(t)}{\mathrm{d}t^2} = \vec{F_i}(t) - \gamma_i m_i \frac{\mathrm{d}\vec{r_i}(t)}{\mathrm{d}t} + \vec{F}_i^R(t) \quad (1)$$

where m_i is the mass, $\vec{r_i}$ is the position of the ion. The interaction between the ion and the surrounding water molecules is approximated by an average frictional force with a friction coefficient $\gamma_i m_i$ (γ_i is the collision frequency) and a stochastic force $\vec{F}_i^R(t)$ resulting from the random collisions. The term $\vec{F_i}(t)$ in Eq. (1) is the systematic force acting on the ith ion. In many simulations, $\vec{F_i}(t)$ is the electric force due to other ions, fixed and induced surface charges and is typically calculated by solving Poisson's equation for the given boundary.

The Langevin equation can be solved by numerical integration at discrete time steps Δt. In the region where $\gamma_i \Delta t \gg 1$, with the assumption that the interparticle force is constant over the integration time step, the following formula is derived [17,18]:

$$\vec{r_i}' = \vec{r_i} + \frac{\vec{F_i}}{m_i \gamma_i} \Delta t + \vec{R_i}(\Delta t) \quad (2)$$

The components of $\vec{R_i}(\Delta t)$ are Gaussian distributions with zero mean and a variance of $2D_i\Delta t = ((2kT)/(m_i\gamma_i))\Delta t$. Eq. (2) is the equation of motion utilized in our model.

2.2. On the Debye–Hückel theory

We will use the Debye–Hückel theory of electrolytes to verify our model. According to the continuum theory, the electrostatic potential around a fixed ion of charge ze can be approximated by a screened Coulomb potential $\phi(r)$, in case of a symmetric two-component electrolyte with a dielectric constant ε_W:

$$\phi(r) = \frac{ze}{4\pi\varepsilon_0\varepsilon_W r} \exp\left(-\frac{r}{r_D}\right) \quad (3)$$

where r is the distance from the fixed ion and r_D is the Debye screening length given by:

$$r_D = \sqrt{\frac{\varepsilon_0\varepsilon_W kT}{2e^2 N_A c(\infty)}} \quad (4)$$

where $c(\infty)$ is the bulk concentration (in mM/l), T is the temperature, N_A is Avogadro's number and k is the Boltzmann constant. Eq. (3) is valid when the Debye length is much bigger than the ion radius. The relation between the electrostatic potential and the concentration of an ion species is:

$$c(r) = c(\infty)\exp(-ze\phi(r)/kT) \quad (5)$$

3. Model and implementation

The electrolyte is modeled in a so-called simulation volume. The electrolyte surrounds a central object, a membrane disk that may hold surface charges and intramembrane dipoles (Fig. 1). The ions move through a continuous medium (water) of homogeneous dielectricity ε_W and viscosity η_W. At the beginning of a simulation, the ions are

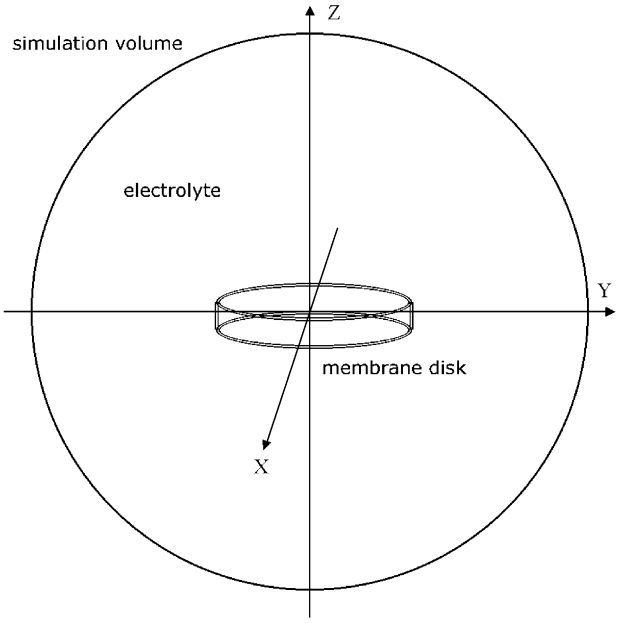

Fig. 1. Schematic representation of the model system. The membrane disk is positioned in the middle of the simulation volume. The space between the disk and the walls of the simulation volume is filled up by the electrolyte. On the upper and lower sides of the membrane disk, surface charges can be placed and an intramembrane dipole can be activated both in the form of uniform charge lattices.

randomly distributed. The next state of the electrolyte (i.e. the new positions of the ions) is always calculated from the previous one. The states are separated by a Δt time interval being much shorter than the simulated process, with the condition of $\gamma_i \Delta t \gg 1$. According to Eq. (2), if only electric forces are present in the system, the displacement of an ion during this Δt is composed of two parts: the electric (Coulomb) and a Brownian part:

$$\Delta \vec{r_i} = \Delta \vec{r_i}^E + \Delta \vec{r_i}^B \tag{6}$$

The Coulomb part summarizes all the effects of the other ions and the membrane charges on the given ion. It can be written in the form:

$$\Delta \vec{r_i}^E = \mu_i q_i \vec{E}(\vec{r_i}) \Delta t \tag{7}$$

where $\mu_i = 1/m_i\gamma_i$ is the mobility of the ion, q_i is the ion charge, $\vec{E}(\vec{r_i})$ is the electric field at $\vec{r_i}$ generated by all the other q_j charges (other ions, surface charges and intramembrane dipoles) present in the system. At the current state of the model, induced charges of ions due to the dielectric heterogeneity caused by the membrane are neglected. This is an approximation based on the fact that the membrane disk is a thin object (5 nm) compared to the mesoscopic volume (approximately 100 nm in diameter) in which the ionic relaxation takes place.

3.1. Geometric aspects, collisions

In our treatment we replace the traditionally used short-range repulsive potentials by geometric concepts to avoid particle overlaps (like ion–ion and ion–membrane overlaps).

The ion is considered as a rigid sphere around the ionic charge, having a radius defined by the following hydrodynamic radius:

$$r_i = \frac{1}{6\pi\eta_W \mu_i} \tag{8}$$

where η_W is the viscosity coefficient of the water.

Ion–ion overlaps are handled by using a stochastic overlap eliminator algorithm which randomly dislocates the overlapping particles. Ion–membrane collisions are modeled by a simple reflection algorithm which reflects the total (electric + Brownian) displacement vectors of the ions on the membrane surface. According to our tests, these algorithms work satisfactorily in the concentration range (< 1 mM) and at the time resolution ($\Delta t = 250$ ps) used in our simulations.

The size of the simulation volume must be large enough to reproduce the physics of the real system. Simulations seem to be sufficiently accurate if the distance between the membrane object and the simulation volume wall exceeds few times (3–4) the Debye length. However, because of performance reasons, the volume size has to be kept at the smallest possible value. As a compromise between the required accuracy and computational cost, the optimal value has to be determined experimentally by carrying out virtual measurements on the modeled electrolyte.

3.2. The diffusive boundary

In our model, the simulation volume is virtually surrounded by a bath of the bulk electrolyte (i.e. constant bath concentration). The walls of the simulation volume are said to be diffusive (or open) because ions can enter and leave the system. This is an essential requirement because typically membranes are charged objects and the electrolyte in the simulation volume must be able to compensate this charge to achieve equilibrium and electroneutrality.

The diffusional contact with the infinite bulk phase is simulated by using a so-called Brown container. The Brown container is an exact copy of the simulation volume created whenever a simulation is started. During a simulation, the electrolytes of the two systems evolve in parallel, with the difference that in the Brown container there is no electric interaction (only Brownian motion) and the walls here are reflective. Anytime a particle in the Brown container collides with the wall, it is reflected and at the same moment a copy of this particle is entered in the simulation volume at the same position. On the other hand, if a particle leaves the simulation volume, it is simply deleted from the list of ions

of the simulation volume (Fig. 2). This simple idea is utilized to simulate the diffusion between the simulation volume and the surrounding infinite bulk phase.

3.3. The simulation algorithm

The algorithm that connects consecutive states of the electrolyte consists of the following operations: (a) precalculation of the ion–ion and ion–membrane Coulomb interactions for each ion in the system (without applying the forces), (b) changing the ion positions according to the stored Coulomb part and by applying the Brownian displacements, (c) handling the ion–membrane collisions, (d) handling the diffusion out of and into the simulation volume (using the Brown container), (e) handling the ion overlaps.

3.4. The simulation tool

The current implementation of the model realizes a simulation system consisting of a simulation volume (shpere or cylinder) containing the electrolyte and a membrane disk in the middle (Fig. 1). The membrane disk can be configured to hold surface charges and intramembrane dipoles (both realized in the form of uniform discrete charge lattices perpendicular to the membrane normal in adjustable depths). The surface charge and dipole configuration of the membrane and various dynamic simulation parameters (time resolution, temperature, interaction switches, etc.) can be changed at arbitrary points of the simulation time course. This offers the possibility to investigate the dynamic behaviour of the electrolyte, such as ionic relaxation processes upon sudden charge reconfiguration of the membrane, as it will be demonstrated.

The simulated system can be investigated visually via the tool's three-dimensional viewer and simultaneously the so-called virtual measuring devices can be used to monitor the system. Three devices are implemented currently: The "dipole moment recorder" records the time trace of the total dipole moment of the electrolyte. The "multipoint concentration recorder" can be used to monitor the time dependence of concentrations of given ion species in one or more measuring spheres having arbitrary radii and locations in the simulation volume. The "spatial concentration and potential profiler" is available for measuring the radial or z-dependence (membrane normal) of ion concentrations and the electric potential generated by the electrolyte.

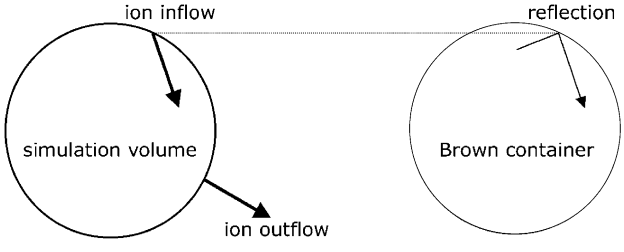

Fig. 2. Handling the diffusion. When an ion in the Brown container hits the volume wall, a copy of it is entered in the simulation volume at the same position. If an ion in the simulation volume hits the volume wall, it is deleted.

The simulations in this work were performed by the simulation tool using its virtual measuring devices (with execution times ranging typically from few hours to few days on an AMD Athlon 1.33 GHz system). Throughout the simulations we used a symmetric electrolyte of Na^+ and Cl^- ions with the following parameters:

Diffusional coefficients: $D_{Na} = 1.33 \cdot 10^{-9} \frac{m^2}{s}$,

$D_{Cl} = 2.03 \cdot 10^{-9} \frac{m^2}{s}$

Ion radii: $r_{Na} = 1.84 \cdot 10^{-10}$ m, $r_{Cl} = 1.21 \cdot 10^{-10}$ m

Bulk concentration: $c = 0.3 \frac{mM}{l}$

Dielectric constant: $\varepsilon_W = 80$,

Viscosity: $\eta_W = 8.91 \cdot 10^{-4} \frac{kg}{m \cdot s}$

Temperature: $T = 298$ K

4. Simulations

4.1. Comparison with the Debye–Hückel theory

The Debye–Hückel theory [19] of the electrolyte offers the possibility of testing the validity of our approach. The first virtual measurements were intended to reproduce the well known equilibrium properties of the electrolyte around a fixed ion, in case of a symmetric two-component electrolyte containing Na^+ and Cl^- ions. (Technically, the fixed ion was realized as a membrane disk having a thickness and diameter equal to the hydrodynamic radius of a Cl^- ion, the negative charge has been realized as a charge positioned in the middle of the disk.) The comparison of our model and the continuum theory was made at the same ion concentration as used later in the dynamic simulations.

The spatial distribution of Na^+ and Cl^- ions has been measured for the modeled electrolyte using a virtual measuring device of the simulation tool (Fig. 3). According to Eq. (5), the electrostatic potential has been derived and by utilizing Eq. (3), the Debye length could be determined by exponential fitting. The bulk concentration was 0.3 mM/l, the radius of the simulation volume (72 nm) was four times the Debye length given by the Debye–Hückel theory. Simulations with time resolutions of 250 ps, 400 ps, 1 ns and 2 ns have been performed at a temperature of 298 K. The Debye lengths obtained from the simulations running at 250 ps, 400 ps and 1 ns time resolutions were in a

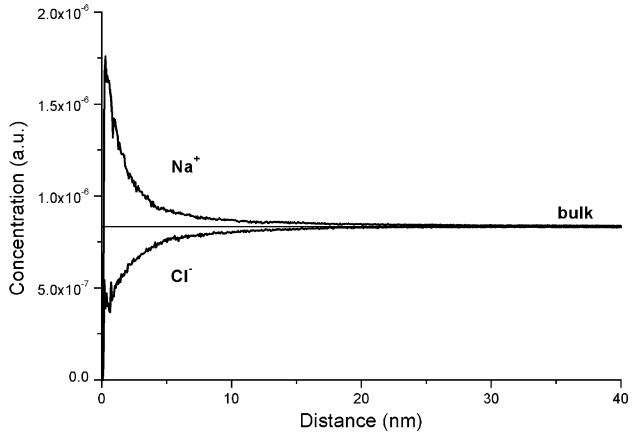

Fig. 3. Simulated Debye–Hückel shielding. The ion concentrations as a function of distance from a fixed negative charge. The electrolyte composition was Na^+ and Cl^- of 0.3 mM/l in bulk, at a temperature of 298 K.

quantitative agreement with the theoretical value. The ratios of the modeled and theoretical values were 1.039, 1.061 and 0.988, respectively.

Note that this shielding behaviour of the electrolyte characterized by the Debye length is actually a dynamic effect: it is the result of the dynamic electric interactions between the ions. Thus the quantitative agreement of the Debye length in the 250 ps—1 ns range implies that the model produces reliable results at these time resolutions. (Above 1 ns there is a drastic decrease of accuracy that can be attributed to the imprecise integration of the electric forces.) Based on this successful test we relied on our model in solving more complicated problems, such as the simulation of the dynamic response of the electrolyte to an intramembrane dipole transition.

4.2. The speed of ionic relaxation

In general, ionic relaxation around biological membranes is of common interest. In particular, we were interested in the kinetics of the relaxation process due to abrupt charge rearrangements inside membrane fragments. This information is utilized for the interpretation of time resolved electric signals of membrane proteins [13] measured by the suspension method [20].

Fig. 4a and b shows the total dipole moment of the electrolyte as a function of time after a sudden intramembrane dipole change. Two cases of intramembrane dipole jumps were investigated: Fig. 4a shows the response of the

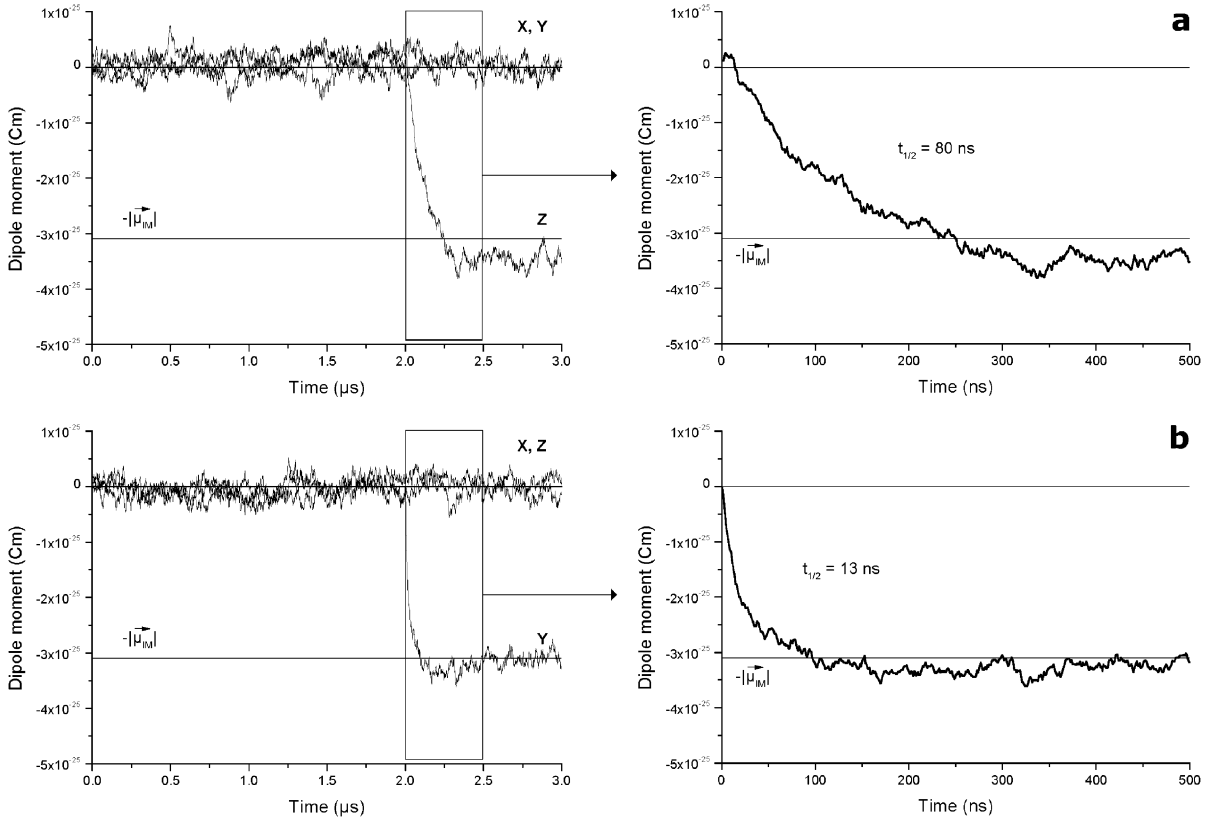

Fig. 4. Simulated electrolyte relaxation. The dipole moment of the electrolyte as a function of time (average of 100 simulations). After the equilibration of the system, at $t = 2$ μs, a rapid intramembrane dipole transition $\vec{\mu}_{IM}$ occurs in the membrane disk. (a) shows the response of the electrolyte in the case of a dipole transition in the direction of the membrane normal (z axis), (b) corresponds to the case of a transition in the membrane plane (y axis). The electrolyte contained Na^+ and Cl^- ions of 0.3 mM/l bulk concentrations, the dimensions of the membrane disk were 50 × 5 nm, and the temperature was 298 K. The $t_{1/2}$ values are half times determined after smoothing with multi exponential fitting.

electrolyte due to a dipole transition in the direction of the membrane normal (*z*-axis), while Fig. 4b displays the case of a dipole transition in the membrane plane (*y*-axis). The data were obtained with the "dipole moment recorder" integrated in the simulation tool. The electrolyte surrounded a membrane disk having a thickness of 5 nm and a diameter of 50 nm in a simulation volume with a diameter of 150 nm. The symmetric electrolyte containing Na^+ and Cl^- ions had a bulk concentration of 0.3 mM/l (Debye length: ca. 18 nm). The surface charge densities of the upper and lower surfaces of the membrane disk were chosen to be in the physiological range, namely -0.04 C/m^2. The surface charges were placed on two uniform lattices with individual charges of 4e, a spacing of 4 nm in a depth of 500 pm measured from the membrane surface. Also the intramembrane dipole was realized in the form of a uniform lattice in the middle of the membrane disk having a total dipole strength of $3.102 \cdot 10^{-25}$ Cm. The separation of the dipole charges were 4 nm and the same lattice spacing and charge magnitudes were chosen as in the case of surface charges. The simulation was performed with a time resolution of 250 ps, at room temperature of 298 K. The total simulation time covered 3 μs, from which 2 μs was used to equilibrate the system, so as to allow the formation of the diffuse double layer around the membrane from the initial random ionic distribution. This buildup process was monitored by an additional virtual measuring device, which recorded the time dependence of the number of Na^+ and Cl^- ions in the simulation volume (Fig. 5). The total number of ions raised from the initial value of 634 to over 1500 during the simulation time course, corresponding to the requirement of electroneutrality. The intramembrane dipole was switched on at 2 μs. In a single simulation, the magnitude of fluctuations of the dipole moment of the electrolyte is much higher than the effect caused by the intramembrane dipole transition. In order to achieve an acceptable signal-to-noise ratio, 100 simulations were performed and averaged for each dipole configuration.

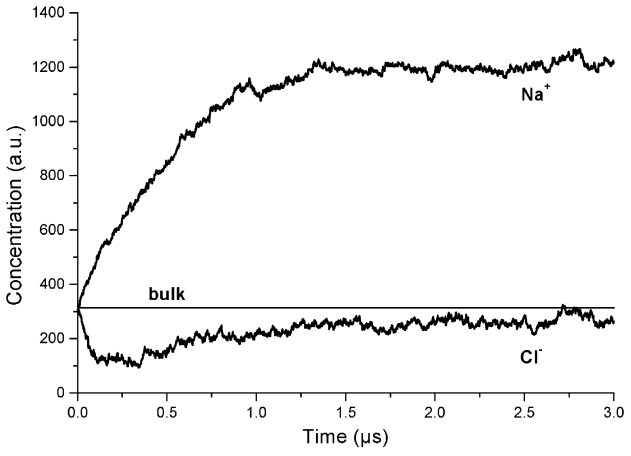

Fig. 5. Buildup of the diffuse double layer. The total number of Na^+ and Cl^- ions in the system recorded as a function of time. At the beginning the ions are randomly distributed. The data correspond to a single simulation.

As it can be seen, the relaxation process corresponding to the y dipole transition is significantly faster. In order to decide whether this effect can be attributed exclusively to the geometry of the membrane, additional simulations were performed with a membrane lacking any surface charges, thus in the absence of the diffuse double layer. As it will be demonstrated later (Fig. 7) also in this case the relaxation kinetics shows an anisotropy, however, the direction dependence is much less pronounced.

In the following, we will present (a) control simulations to verify the used time resolution and size of the simulation volume, (b) the dependence of the relaxation kinetics on the geometric details of the intramembrane dipole lattice, (c) the linearity of the response of the electrolyte, and (d) the anisotropy of the ionic relaxation. For the sake of simplicity and because of performance reasons, the simulations were performed with membrane disks having no surface charges, and the initial linear phase of the relaxation kinetics was used to characterize the speed of the process.

4.3. Control simulations

There are simulation parameters that have to be chosen based on empirical and practical considerations: the simulation time step and the radius of the simulation volume. Using a smaller time step or a larger radius means improved accuracy but requires more calculation time. The optimal values have to be determined as a compromise between the required accuracy and the computational cost.

The upper limit on the time step is introduced because the electric interactions between the ions and the charged membrane object have to be simulated with a satisfying accuracy. The optimal value can be determined directly by carrying out simulations with different time resolutions and by comparing the relaxation kinetics. The early 100 ns of the relaxation process can be considered to be linear (see Fig. 7, case A) so the initial slopes of the relaxation kinetics measured at the different time resolutions can be compared directly after linear fitting. Fig. 6 shows the slopes of the relaxation kinetics measured with time resolutions in the range of 100 ps–10 ns. As it can be seen the slope values start to deviate from the reference line at 1 ns, in concert with the simulations performed for a comparison with the Debye–Hückel theory. In the <1 ns range the values are nearly identical meaning that a time step of 250 ps is a reasonable choice. The time resolution of 250 ps in our simulations may seem rather rough compared to the values reported in many papers utilizing Brownian dynamics. This is due to the facts that (a) we use a relatively low concentration range and (b) the relaxation process takes place in a mesocopic volume. Because of these, the displacements of the ions during the time step is small enough compared to the typical ion–ion and ion–membrane distances, so the electric interactions are calculated at a proper precision level.

The validity of the chosen radius of the simulation volume has been verified too. Three independent simulation

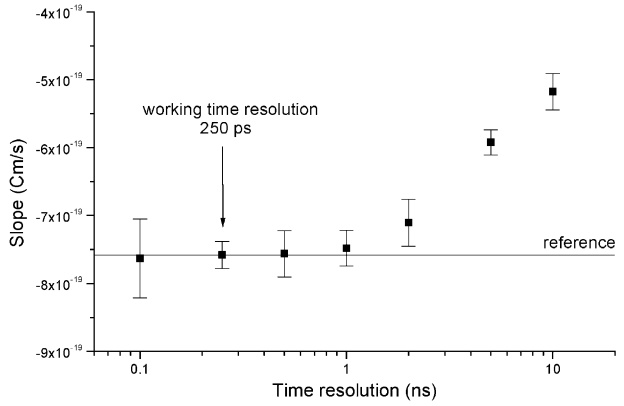

Fig. 6. Verification of the time resolution. The first 100 ns of the relaxation kinetics (i.e. the dipole moment of the electrolyte as a function of time) is recorded at time resolutions in the 100 ps–10 ns range and the slopes (of the dipole moment function of the electrolyte) based on linear fitting are shown (with standard deviations). At a given time resolution there are five independent slope measurements based on the average of 4000 simulations each (except for the 100 ps case with 2000 simulations). The reference line is defined by the mean value of the slopes measured at 250 ps.

series each consisting of 2000 simulations have been performed at a simulation volume diameter of 200 nm. This corresponds to a simulation volume more than the double of the original system. Also in this control system the results (obtained from linear fitting of the first 100 ns of the relaxation kinetics) were within error compared to the reference system (data not shown).

4.4. Insensitivity to intramembrane details

In the foregoing, the intramembrane dipole was realized in the form of a uniform lattice placed in the middle of the membrane disk. A question can be asked whether the particular realization of the intramembrane dipole lattice affects the relaxation kinetics. If yes, how? As it will be demonstrated, the relaxation kinetics does not show any significant dependence on the geometric details of the intramembrane dipole lattice. Fig. 7 shows six different cases (A, B, C, D, E and F) of the intramembrane configuration. In cases A, B, C, D, E the intramembrane dipole is parallel with the membrane normal, in case F it is perpendicular to it. Situation A, B, C, D correspond to the same lateral dipole density (,thus total intramembrane dipole strength) but each of them has a different lattice geometry. Situation A is the original configuration (the lattice is placed in the middle of the membrane with a lattice spacing of 4 nm, the separation between the dipole charges of magnitude 4 e is 4 nm). In situation B the separation between the individual dipole charges is reduced (25%) while maintaining the dipole strength. In situation C the dipole lattice of B is shifted by 1.5 nm in the direction of the membrane normal. In D, the lattice spacing has been decreased (50%) while maintaining the lateral dipole density. It is apparent from the figure that the relaxation kinetics is insensitive to the intramembrane configurations A, B, C and D. This can also be explained by the mesoscopic nature of the system. The ions involved in this process are distributed around the membrane in a relatively large volume. Typical distances between the ions and the membrane are large compared to the structural changes between the different intramembrane configurations. Similarly to the case of the intramembrane dipoles, the geometric details of the surface charge lattices are also irrelevant when investigating the relaxation kinetics under the present circumstances.

4.5. Linearity

We tested how the relaxation kinetics depends on the magnitude of the intramembrane dipole. Case E in Fig. 7 has

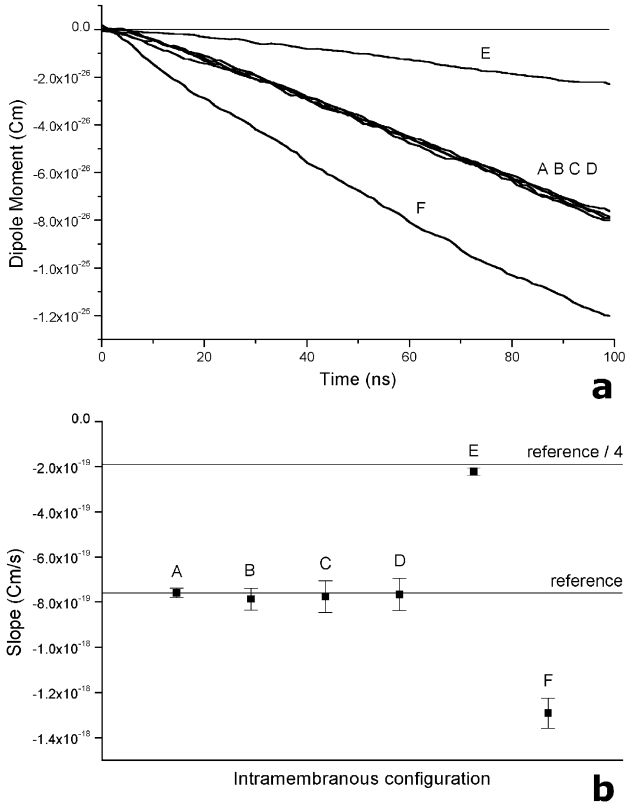

Fig. 7. Intramembrane dipole configurations. For six different intramembrane dipole configurations the first 100 ns of the relaxation kinetics (i.e. the dipole moment of the electrolyte as a function of time) is recorded (a) and the slopes (of the dipole moment function of the electrolyte) are shown (with standard deviations) (b). At a given configuration there are 5 independent slope measurements each based on a linear fit using the average of 2000 simulations (except E where 16,000 simulations are averaged), (a) shows the data obtained by averaging all five simulation series per configuration. In cases A, B, C, D and E the intramembrane dipole moment is parallel with the membrane normal, in case F the dipole moment is perpendicular to the membrane normal. The lateral density of the intramembrane dipole moment is the same in all cases, except E (25%). The cases A, B, C and D differ only in the particular realization of the same lateral dipole density. The reference line is defined by the mean value of the slopes measured in case A. (For further details see text.)

the same lattice properties as case A, except that the magnitude of dipole charges and so the lateral dipole density, i.e. the strength of the total dipole is smaller (25%). The results show that the response of the electrolyte to an intramembrane dipole change of magnitude μ_{IM} is in first approximation linear in the sense that for the dipole function $\mu(t)$ of the electrolyte we can write:

$$\mu'_{IM} = \alpha \cdot \mu_{IM} \Rightarrow \mu'(t) = \alpha \cdot \mu(t) \quad (9)$$

We note that the range of the dipole strength where the linearity was investigated covers the physiological range. (For the sake of visualization, the intramembrane dipole lattice used in case A can be transformed into a lattice where the positive and negative unit charges of a dipole are separated by 1 nm and the lateral distance between the dipoles is also 1 nm.)

4.6. Anisotropy

In case F (Fig. 7) the lateral dipole density is the same as in case A but the direction of the intramembrane dipole is perpendicular to the membrane normal. As it is apparent from the figure, the ionic relaxation is faster in this direction (y). The ratio of the slopes in the initial phase of the ionic relaxation is approximately 1.67. Obviously, this ratio depends on the radius of the membrane disk (for a very small membrane the kinetic anisotropy has to disappear). As it was presented earlier, when the diffuse double layer is present the ratio is considerably higher (close to 5, see Fig. 4). So we can say that already in the bulk electrolyte there is an anisotropy in the relaxation kinetics that is significantly enhanced if the diffuse double layer is present around the membrane disk.

5. Discussion

5.1. Relevance to the theory of the suspension method

The suspension method is a technique offering the unique possibility to follow the intramolecular charge rearrangements of membrane proteins in three dimensions [14]. The interpretation of the experimental results is based on a theory [13] that uses certain assumptions for the ionic relaxation processes around membrane fragments. The suspension method was originally developed for investigating the operation of bacteriorhodopsin (bR), the simplest ion pump in biology.

The suspension method works with a macroscopic number of oriented membrane fragments containing the membrane proteins and suspended in an electrolyte (e.g. for bR, the purple membrane fragments are oriented by electric and/or magnetic fields). The membrane fragments are disk-like particles of different diameter. During their operation, the protein molecules undergo conformational transitions between certain intermediates (e.g. having been triggered by light, the bR pumps a proton across the membrane while going through the photocycle).

Based on the simulations we determined the half time of the relaxation process in the case of a membrane disk with an intramembrane dipole lattice. Since the relaxation kinetics did not change upon decreasing the lattice spacing (case D in Fig. 7), we can say that our discrete lattice is a good approximation for a continuous and homogeneous dipole distribution (referred later as the ‘‘continuous disk’’). On the contrary, in typical applications of the suspension method, a conformational transition is a rare event in a given membrane fragment on the time scale of the relaxation process, so here we are dealing only with local changes in the intramembrane dipole.

However, it can be conceded that the properties of the relaxation kinetics (anisotropy, linearity and insensitivity to intramembrane details) investigated in the present simulations can be applied for the case of real samples used by the suspension method.

Without getting into detail, let us only consider the initial phase of the relaxation kinetics and define the speed of the process by the ratio of the initial slope of the dipole moment function of the electrolyte and the magnitude of the intramembrane dipole. Based on the superposition principle, the speed of the relaxation kinetics obtained for the ‘‘continuous disk’’ is an average value that corresponds to a macroscopic number of conformational transitions occurring on random locations on different membrane disks (of the given disk diameter). The superposition principle can be applied as long as the perturbation in the spatial distribution of the ionic cloud around the membrane caused by the intramembrane dipole change is negligible. This holds both for the case of local dipole changes in real samples and for the initial phase of the relaxation process for the ‘‘continuous disk’’. Hence, it is plausible to assume that the conclusions drawn from the simulated initial phase of the relaxation can be extended to the whole time scale of the real process.

An important assumption of the theory of the suspension method is that the transient intramembrane dipoles (accompanying the conformational transitions between the intermediates) are rapidly compensated by the sorrounding electrolyte (with relaxation time t_R) compared to the life time of the investigated intermediate states (t_L):

$$t_R \ll t_L \quad (10)$$

We simulated the relaxation process and know its speed in a particular situation (bulk concentration and disk size). This can be used as a qualitative upper estimate for systems having higher bulk concentrations (where the relaxation is faster) and other membrane sizes or size distributions. In a particular situation of given life times of intermediate states (i.e. in the time range under investigation), the validity of the above relation should be verified. (For measurements on bR, the life times of the investigated intermediates are on the

μs and ms time scale, therefore relation (10). obviously holds.)

In addition to relation (10), there are two assumptions of the theory of the suspension method: (a) the response of the electrolyte to an intramembrane dipole change is linear and (b) the particular realization of the intramembrane dipole change (the locations of charge movements inside the membrane protein) does not affect the relaxation kinetics. As it was demonstrated previously, these assumptions are confirmed by our simulations. Based on these conditions, the theory of the suspension method renders possible to conclude on the intermediate dipole moments $\mu_i^k (k=x,y,z)$ based on macroscopically detectable $u^k(t)$ voltages:

$$\mu^k(t) \sim \sum_i \mu_i^k \frac{\mathrm{d}}{\mathrm{d}t} x_i(t) \tag{11}$$

where $x_i(t) - s$ are the concentrations of the intermediates (obtained from absorption kinetics measurements in the case of bR). The quantities $\mu^k(t)$ have to be derived using the formula:

$$u^k(t) \sim \sum_l \mu^k(t) \cdot f^{lk} \tag{12}$$

Here the f^{lk} coefficients can be calculated from the orientational distribution of the molecules. If it is possible to create situtations experimentally (by changing the symmetry properties of the sample, e.g. by orientation with electric/magnetic fields, photoselection) from which one or more of the $\mu^k(t) - s$ can be obtained using Eq. (12), then it is possible to calculate the corresponding μ_i^k intermediate dipole moments based on Eq. (11). The interpretation of the μ_i^k values is not a trivial task requiring some additional considerations [13]. For instance, the anisotropy of the relaxation kinetics implies that the membrane in-plane components ($\mu^x(t)$ and $\mu^y(t)$) of the electric signals measured by the suspension technique appear with a significantly lower weight than the normal $\mu^z(t)$ component, due to the much stronger screening of the electrolyte in these directions. This should be taken into account when using the results obtained by the suspension method to check the validity of certain intermediate structures suggested by molecular dynamic models [15].

Finally, we note that our simulations were performed at a low bulk concentration compared to the physiological value. The suspension method when used for the detection of electric signals in three dimensions requires low salt concentrations. In the case of bR, although it works at high salinity under natural conditions, the function of the protein is preserved also in this low concentration regime (e.g. 0.3 mM/l used in the present simulations).

5.2. Concluding remarks

The model has been verified by a comparison with the Debye–Hückel theory and by performing direct control simulations to validate the used time resolution and simulation volume radius. Simulations were performed to record the response of the electrolyte upon fast intramembrane dipole transitions and the half times of the relaxation processes could be determined. We demonstrated that around a membrane disk the relaxation kinetics has its characteristic anisotropy. This is already present in the bulk electrolyte (in the case of a membrane disk without surface charges) and it is further increased by the anisotropy of the diffuse double layer. We showed that the response of the electrolyte to the dipole transition is with good approximation linear and that the particular details of the intramembrane dipole do not affect the kinetics.

The kinetics of the ionic relaxation is an important factor in quantifying the electric signals of membrane proteins (e.g. ion transporters) measured in three dimensions by the suspension method. The properties of the relaxation process (speed, anisotropy, linearity and insensitivity to the intramembrane dipole details) investigated in this work, validate the assumptions of the theory of the suspension method and are in agreement with available electric experiments [14–16]. As a result of a complex evaluation procedure based on the theory [13], it is possible to conclude on intramolecular charge displacements in three dimensions, associated with the conformational changes accompanying the operation of the protein studied. Using this information one can establish a preference among molecular dynamics models [15]. We note that besides bR, the suspension method has also been applied to investigate other ion pumps and light sensitive proteins (e.g. the Cl-pumping halorhodopsin, octopus rhodopsin, photosystem-I) [21–26].

Given the flexible architecture of our simulation tool, it is straightforward to extend it in several directions. Additional virtual devices (e.g. for particle tracking, ionic flux recording, electric potential scanning) can be added to the simulation tool if required later. Some potential areas of development are: (a) modeling biomembrane-electrolyte systems of higher geometric complexity, (b) simulating complex electrolytes, buffer effects [27], (c) functional integration of ion channels, ion pumps and specific binding ports, (d) calculating the structure of the electric field in the electrolyte near specific biomembrane charge patterns (e.g. supramolecular assemblies). In general, the corpuscular nature of this mesoscopic dynamic model and the flexibility of the implementation offers the possibility of investigating many new aspects of membrane coupled energy conversion processes.

Acknowledgements

This work was supported by a grant of the Hungarian research foundations: OTKA T-029814. Many thanks to Laszlo Fabian for his assistance in simulation management. We are also indebted to Pal Ormos for helpful discussions.

References

[1] B. Roux, Molecular dynamics simulations of ion channels: how far have we gone and where are we heading? Biophys. J. 74 (1998) 2744–2745.

[2] P. Lauger, H. Apell, Jumping frequencies in membrane channels: comparison between stochastic, molecular dynamics and rate theory, Biophys. Chem. 16 (1982) 209.

[3] E. Jakobsson, S.W. Chiu, Stochastic theory of ion movement in channels with single-ion occupancy. Application to sodium permeation of gramicidin channels, Biophys. J. 52 (1987) 33–45.

[4] S.H. Chung, M. Hoyles, T. Allen, S. Kuyucak, Study of ionic currents across a model membrane channel using Brownian dynamics, Biophys. J. 75 (1998) 793–809.

[5] S.C. Li, M. Hoyles, S. Kuyucak, S.H. Chung, Brownian dynamics study of ion transport in the vestibule of membrane channels, Biophys. J. 74 (1998) 37–47.

[6] T. Schirmer, P. Phale, Brownian dynamics simulation of ion flow through porin channels, J. Mol. Biol. 294 (1999) 1159–1168.

[7] W. Im, S. Seefeld, B. Roux, A grand canonical Monte Carlo-Brownian dynamics algorithm for simulating ion channels, Biophys. J. 79 (2000) 788–801.

[8] R.C. Wade, B.A. Luty, E. Demchuk, J.D. Madura, M.E. Davis, J.M. Briggs, J.A. McCammon, Simulation of enzyme-substrate encounter with gated active sites, Nat. Struct. Biol. 1 (1994) 65–69.

[9] J.D. Madura, J.M. Briggs, R.C. Wade, M.E. Davis, B.A. Luty, A. Ilin, J. Antosiewicz, M.K. Gilson, B. Bagheri, L.R. Scott, J.A. Mccammon, Electrostatics and diffusion of molecules in solution—simulations with the University of Houston Brownian Dynamics program, Comput. Phys. Commun. 91 (1995) 57–95.

[10] A.H. Juffer, J. de Vlieg, P. Argos, Adsorption of proteins onto charged surfaces: a Monte Carlo approach with explicit ions, J. Comput. Chem. 17 (1996) 1783–1803.

[11] G. Moy, B. Corry, S. Kuyucak, S.H. Chung, Tests of continuum theories as models of ion channels: I. Poisson–Boltzmann theory versus Brownian dynamics, Biophys. J. 78 (2000) 2349–2363.

[12] B. Corry, S. Kuyucak, S.H. Chung, Tests of continuum theories as models of ion channels: II. Poisson–Nernst–Planck Theory versus Brownian dynamics, Biophys. J. 78 (2000) 2364–2381.

[13] L. Oroszi, A. Dér, P. Ormos, Theory of electric signals of membrane proteins in three dimensions, Eur. Biophys. J. 31 (2002) 136–144.

[14] A. Dér, P. Ormos, Introduction of a method for three-dimensional mapping of the charge motion in bacteriorhodopsin, Biophys. Chem. 56 (1995) 159–163.

[15] A. Dér, L. Oroszi, A. Kulcsár, L. Zimányi, R.T. Boconádi, L. Keszthelyi, W. Stoeckenius, P. Ormos, Interpretation of the spatial charge displacements in bacteriorhodopsin in terms of structural changes during the photocycle, Proc. Natl. Acad. Sci. 96 (1999) 2776–2781.

[16] L. Keszthelyi, P. Ormos, Protein electric response signals from dielectrically polarized systems, J. Membr. Biol. 109 (1989) 193–200.

[17] D.L. Ermak, A computer simulation of charged particles in solution: I. Technique and equilibrium properties, J. Chem. Phys. 62 (1975) 4162–4196.

[18] W.F. van Gunsteren, H.J.C. Berendsen, Algorithms for Brownian dynamics, Mol. Phys. 45 (1982) 637–647.

[19] P. Debye, E. Hückel, Zur Theorie der Elektrolyte, Physik. Zeitschr. 24 (1923) 185–206.

[20] L. Keszthelyi, P. Ormos, Electric signals associated with the photocycle of bacteriorhodopsin, FEBS Lett. 109 (1980) 189–193.

[21] A. Dér, K. Fendler, L. Keszthelyi, E. Bamberg, Primary charge separation in halorhodopsin, FEBS Lett. 187 (1985) 233–236.

[22] A. Dér, S. Száraz, L. Keszthelyi, Charge displacements during the photocycle of halorhodopsin, J. Photochem. Photobiol. B. 15 (1992) 299–306.

[23] E. Govorunova, A. Dér, R. Tóth-Boconádi, L. Keszthelyi, Photosynthetic charge separation in oriented membrane fragments immobilized in gel, Bioelectrochem. Bioeng. 38 (1995) 53–56.

[24] P. Ormos, A. Dér, S. Száraz, Zs. Tokaji, L. Zimányi, K. Nagy, Photoreactions and related charge displacements in the rhodopsin from *Sepia officinalis*, J. Photochem. PhotoBiol. B. 35 (1996) 7–12.

[25] K. Ludmann, G. Ibron, J.K. Lanyi, G. Varo, Charge motions during the photocycle of pharaonis halorhodopsin, Biophys. J. 78 (2000) 959–966.

[26] M. Lakatos, G.I. Groma, C. Ganea, J.K. Lanyi, G. Varo, Characterization of the azide-dependent bacteriorhodopsin-like photocycle of salinarum halorhodopsin, Biophys. J. 82 (2002) 1687–1695.

[27] R. Tóth-Boconádi, A. Dér, L. Keszthelyi, Buffer effects on electric signals of light-excited bacteriorhodopsin, Biophys. J. 78 (2000) 3170–3177.